# ICE BREAKING AND SHIP MODELLING

**Karl-Heinz Rupp**
*Hamburg, Germany*

**Keywords:** Ice breaking, Hull shape, Ice thickness, Friction, Resistance astern, Stability control, Ice floes, ice cake, brash ice, Rafted ice, modulus of elasticity, Propulsion

## Contents

## 1. Introduction

In this chapter the ice breaking process and the ice resistance of a ship in level ice are described. The ice resistance includes the ice breaking at the waterline, the submerging of the broken ice pieces and the resistance of the broken ice along the hull. When ice hits a propeller nozzle additional resistance occurs. The milling of ice with the propeller increases the propeller torque and therefore also the required power.

In the second section ship model tests in ice are described. Model tests are important for getting information on the performance of the ice breaking ship design. The results of the ice model tests confirm whether the performance of the design is acceptable or if modifications are necessary. Model tests help to reduce or to avoid shortcomings in the ship design.

Similarity laws and the conversion from model scale to full scale are explained for different ice conditions. The tests of ship models in model ice can be conducted in different ways, both in the handling and in the powering of the ship model. In addition to the data measured during ice model tests also the observations of the model test both above and particularly below the water surface are very important. All important maneuvers from the future operational profile of the icebreaking ship can be conducted in model scale for the optimization of the design.

## 2. Ice Breaking Process in Level Ice and Other Ice Conditions

When a ship sails in level ice the total resistance of the ship is the sum of the following components (Figure 1): Ice breaking at the waterline, the turning phase of the broken ice cusp, submerging of the ice, the movement of the broken ice pieces along the hull and the water resistance. Behind the ship some of the broken ice pieces and crushed ice float in the channel and some of the ice has been pushed underneath the unbroken level ice

(ice clearing aside). The propeller-ice-interaction shown in Figure 2 does not influence the resistance in ice but instead causes an increase in propulsive power.

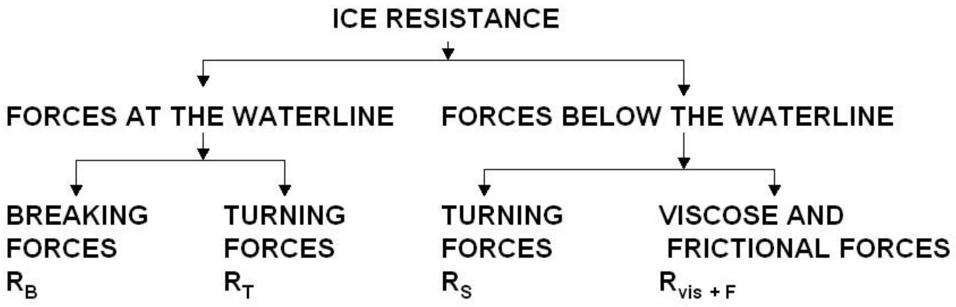

Figure 1. Division of ice resistance into components

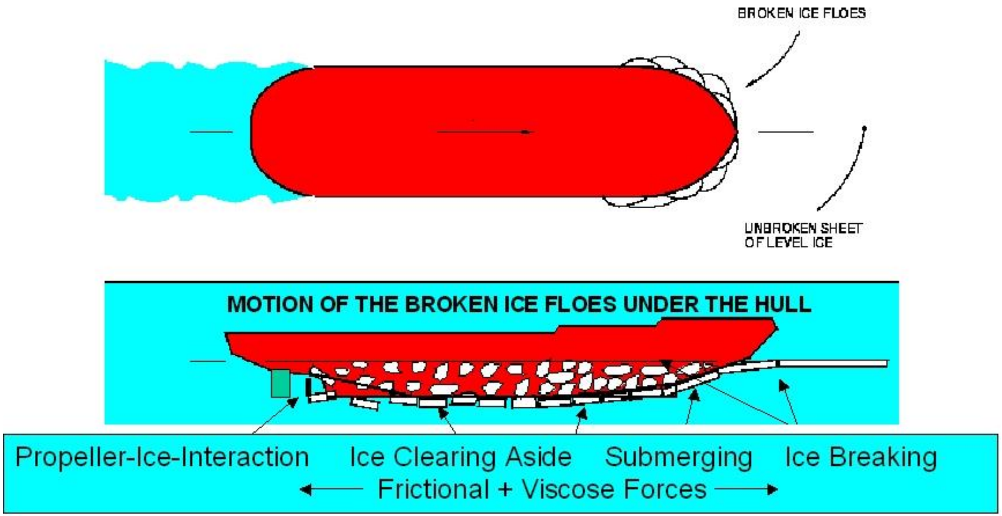

Figure 2. Ice resistance components in level ice (HSVA)

## 2.1. Ice Breaking and Turning of the Cusps

When an icebreaking ship enters the ice sheet the following occurs: In the first moment of contact the ice cannot carry the load from the stem and is crushed until, with deeper penetration, the contact area is large enough to transfer the vertical forces from the ship to the level ice. The crushing phenomenon occurs when the local stress is high enough to crush the ice but does not exceed the bending strength of the level ice. From the crushed ice at the stem both radial and circular cracks arise in the ice (Figure 3). With increasing vertical forces from the stem the ice deflects until failure occurs. The first half-moon shaped ice pieces (cusps) break off when the stress condition in the ice exceeds the bending strength. The cusps break free from the unbroken level ice and start to turn. At the end of the turning process the cusps are smashed against the shell and may break into smaller triangular pieces. The breaking of further new cusps occurs in a similar way around the bow when sailing ahead (Figure 4). Circular cracks usually form from ships with V-shaped bow and approximately rectangular ice cusps from ships with a landing craft type bow shape (e.g. the Thyssen/Waas bow).

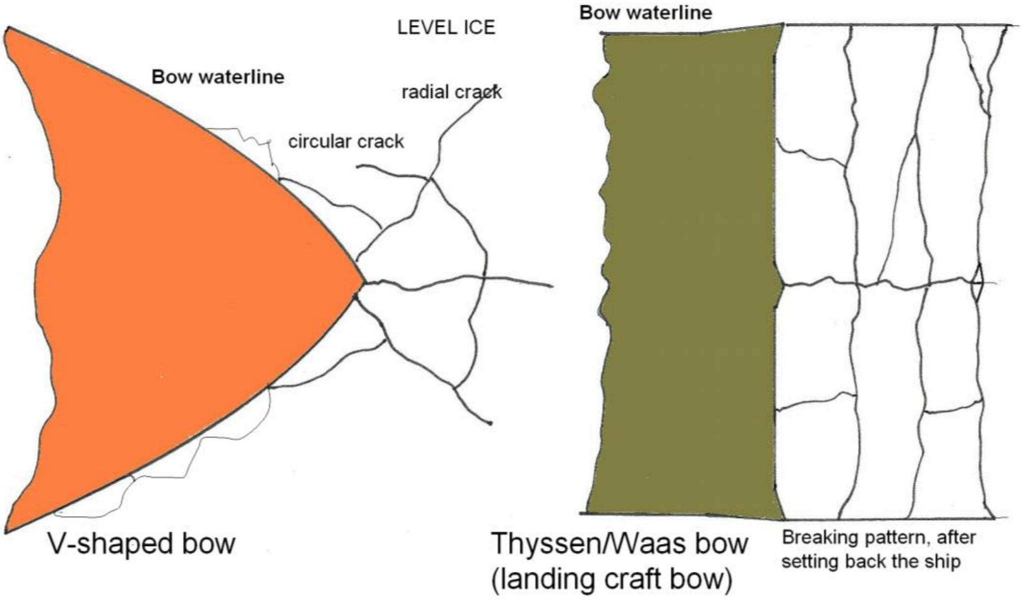

Figure 3. Icebreaking pattern at the stem: V-shaped and rectangular waterline

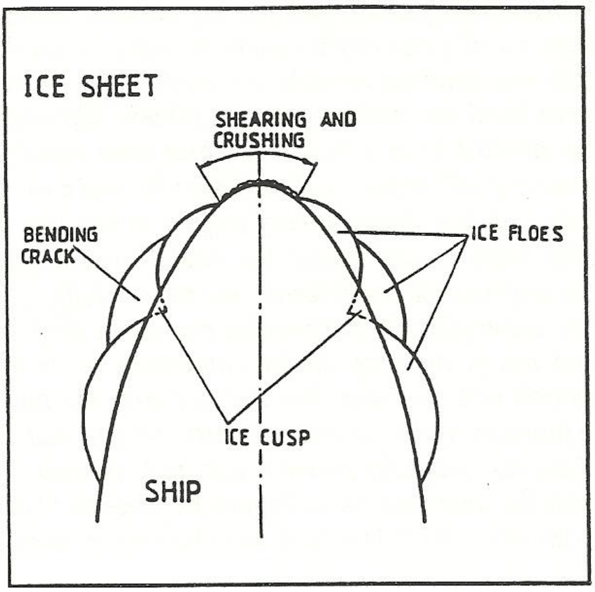

Figure 4. Idealized breaking pattern (Enkvist, Varsta and Riska 1979)

The forces due to breaking the ice in the waterline with a simplified 2-D bow form can be calculated to be:

$$F_N(t) = F_Z(t)/\cos\phi$$

$$\mu F_N(t) = \mu F_Z(t)/\cos\phi$$

$$F_X(t) = F_N(t)\sin\phi + \mu F_Z(t)\cos\phi$$

$$\rightarrow F_X\left(t\right) = F_Z\left(t\right)\left(\tan\phi + \mu\right)$$

Where

$F_X\left(t\right)$ : Horizontal force ( = ice resistance)

$F_{\mathrm{N}}\left(t\right)$: Normal force between the edge of the ice floe and the hull plating

$\mu$ : Dynamic friction coefficient

$F_Z\left(t\right)$: Vertical force

$\phi$: The stem angle with horizontal

$t$: Time

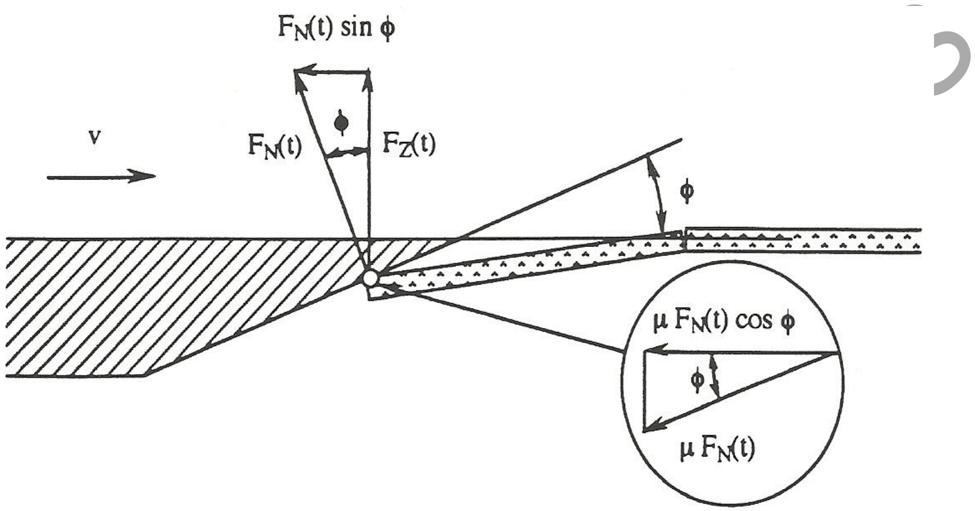

Figure 5. Hull ice interaction forces at the waterline and slightly below in the ice flow turning zone (Kämäräinen 1993)

The ice breaking process is illustrated in Figure 6. The stress distribution in the level ice is shown in Figure 7. Darker color highlights areas of higher stress which define the half-moon shaped cusps.

The point of contact between the bow and the unbroken level ice changes its position with time. Outgoing from the contact point a circular crack breaks the cusp off. The contact point for the next cusps shifts to a position where the ends of the previous cusps meet (Figure 5).

Calculations of the resistance in ice show the distribution of the ice breaking resistance over the beam of the ship for low, medium and high speed (Figure 8). The calculated ice breaking resistance over the ship's breadth at varied speed shows the effect of the dynamic contributions. Kayo (1993 performed ice model tests with a segmented bow model of an icebreaking vessel. The measured loads distributions are similar to the calculated load distribution in Figure 8.

The local angle of attack at the waterline is usually largest at the stem and becomes smaller when moving along the hull from the stem to the flat of side. This means that more favorable angles for breaking the ice by bending can be found in the forward part of the bow. When moving further outboard (and aft) the effective ice breaking angles become smaller until in way of the shoulder only crushing of the ice is possible. In particular the breaking mode of the final cusp at the ship’s beam dictates whether the ship can move through a broken channel or if the shoulder must crush the ice.

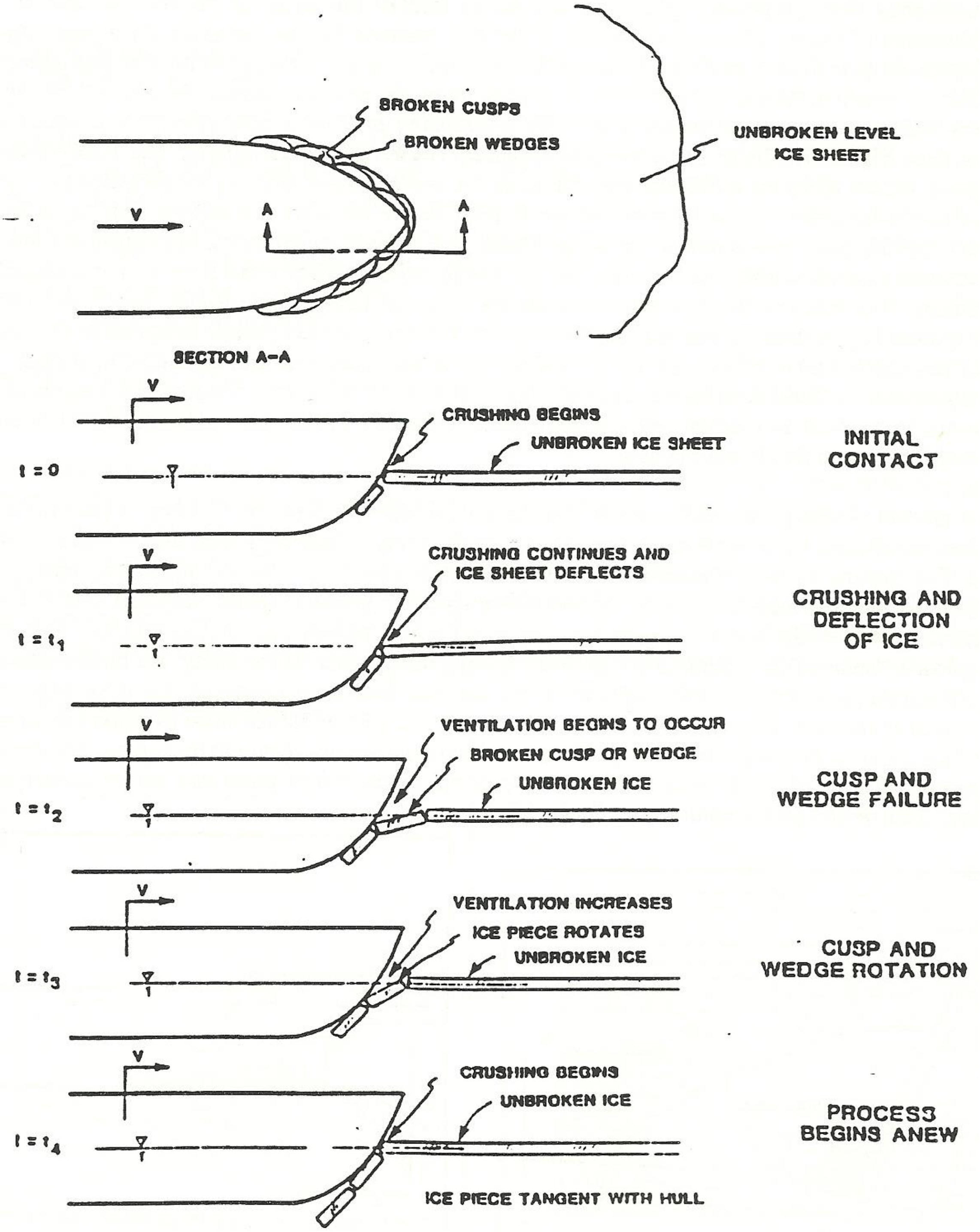

Figure 6. Ice breaking process at the waterline (Kotra, Baird and Naegle 1983)

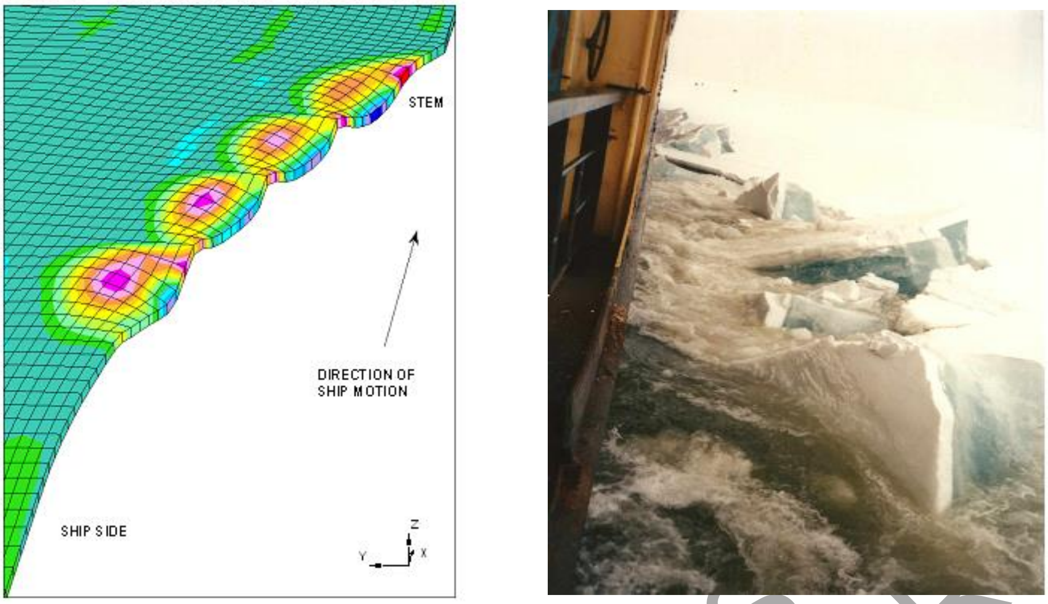

Figure 7. Montage of the non-simultaneous floe failures covering the ship waterline from the stem to amidships: Principal stress distribution on the ice cover shown for purpose of illustration only (Valanto 2001, Valanto 2013), Photo HSVA

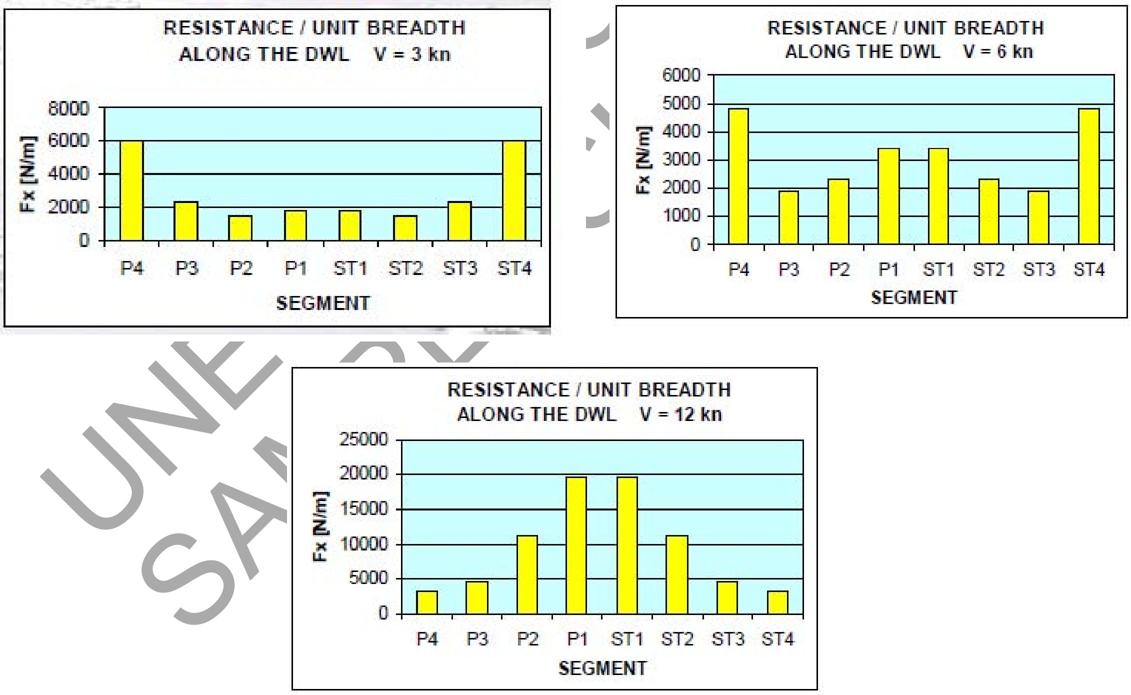

Figure 8. Distribution of the ice resistance at the waterline over the ship breath at low, medium and high speed (Valanto 2001)

## 2.2. Ice Submerging Forces

After the ice has been broken and the cusps have rotated, the cusps slide along parallel to the hull. The ice is broken into pieces which together cover the hull. The bow area is covered with a mosaic of broken ice pieces. In the keel area ice may slide to the side. The photo series of a model test in level ice (Figure 9) shows the ice around a ship.

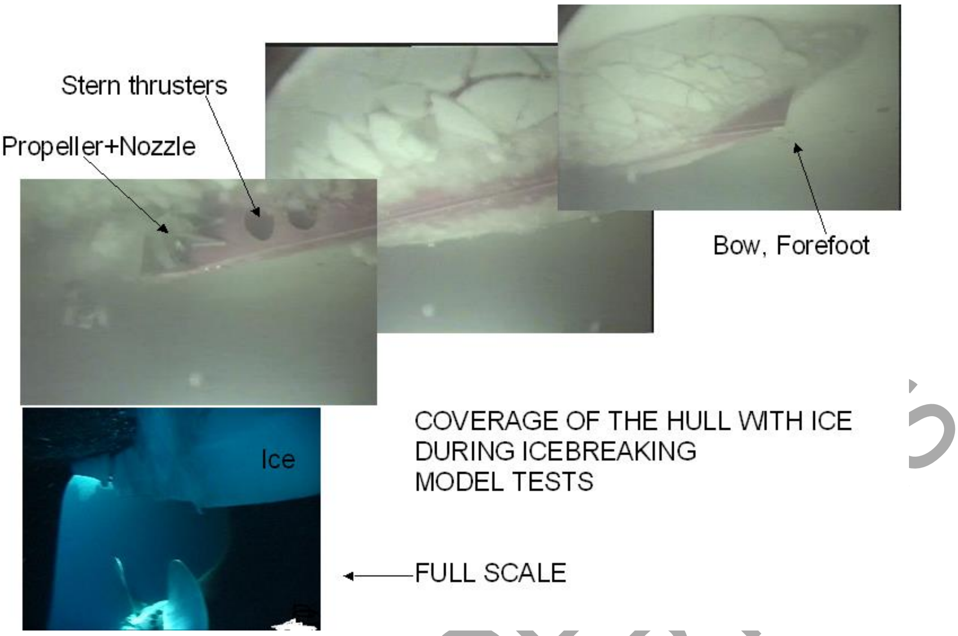

Figure 9. Breaking of level ice, ice below the water level at the hull (Photos HSVA)

Resistance to the ship motion is caused by friction between the hull and the snow + ice piece as well as the normal force due to buoyancy of ice piece plus snow. In Figure 10 the ice resistance due to normal forces in the ice submersion phase for a 2-D bow shape is described.

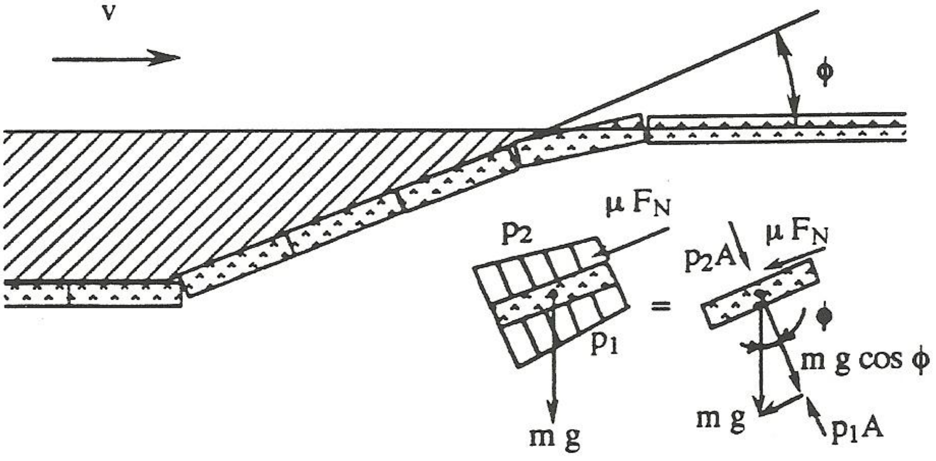

Figure 10. Ship-ice interaction forces in ice submersion phase (Kämäräinen 1993)

From Kämäräinen 1993, page 15: “The normal force due to the ice buoyancy is now

$$F_N = p_1 A - p_2 A - mg\cos\phi \tag{1}$$

Where

$F_N$ : Normal force between the ice floes and hull plating
$p_1$ : Hydrostatic pressure below the ice floes
$p_2$ : Hydrostatic pressure above the ice floes
$A$ : The area of the ice floes in the bow area
$m$ : The weight of the ice in the bow area

and the resistance due to the normal force is

$$R_N = F_N \sin\phi + \mu F_N \cos\phi \qquad (2)$$

Now $A = TB/\sin\phi$
$p_1 - p_2 = \rho_W \, g \, h_{ICE} \cos\phi$ and
$m = \rho_{ICE} h_{ICE} \, TB/\sin\phi$

where
$h_{ICE}$ : Ice thickness
$T$ : Draft of the vessel
$B$ : Beam of the vessel
$\rho_W$ : Density of water
$\rho_{ICE}$ : Density of ice

The following equation is for the ice resistance due to the normal forces in the ice submersion phase

$$R_N = (\rho_\Delta \, g \, h_{ICE} \, T \, B) \, (\cos\phi + \mu \cos\phi / \tan\phi) \qquad (3)$$

where $\rho_\Delta$ is the difference between water and ice density $(= \rho_W - \rho_{ICE})$

Kämäräinen 1993 page 16:
“The tangential buoyancy force along the hull surface causes an interaction force between the ice breaking and turning forces and the ice submerging force. It can be written for the tangential buoyancy force (see Figure 11)

$$F_T = p_1 A_C - p_2 A_C - mg \sin\phi \qquad (4)$$

where
$F_T$ : Tangential force along the hull plating due to ice buoyancy
$A_C$ : Cross section of the floes in the bow area
$p_1$ : Hydrostatic pressure at the lower end of the ice floes
$p_2$ : Hydrostatic pressure at the upper end of the ice floes

For a 2-D hull form

$p_1 - p_2 = \rho_W \, g \, T$
$A_C = h_{ICE} \, B$ , and
$m = \rho_{ICE} h_{ICE} \, TB / \sin\phi$

the tangential force due to the submerged ice floes

$$F_T = \rho_\Delta \, g \, h_{ICE} \, BT \qquad (5)$$

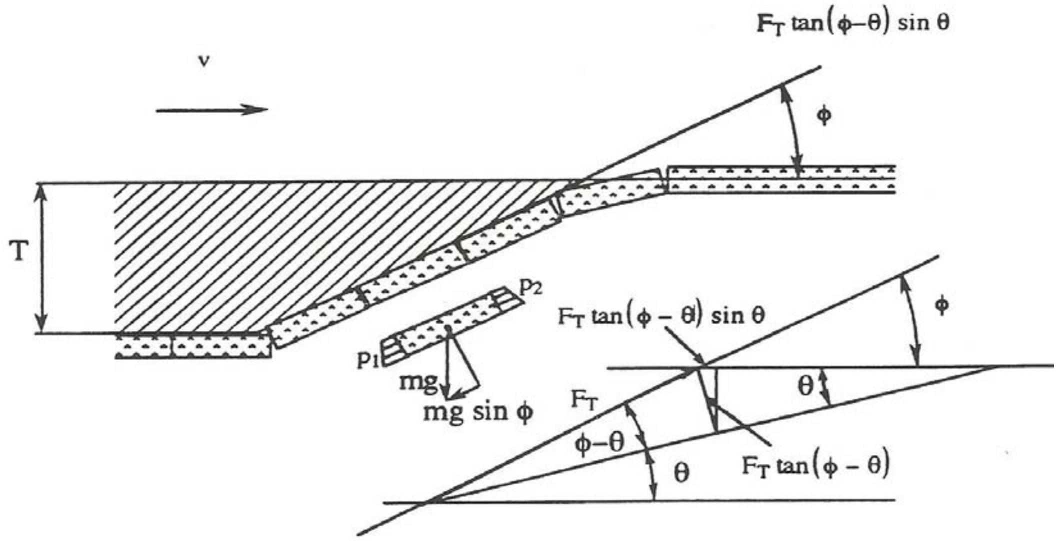

Figure 11. Interaction forces between the forces at the waterline level and the ice submerging forces (Kämäräinen 1993)

From Figure 11 we can see that most of the tangential forces $F_T$ are transmitted to the ice field. A normal force $F_T \tan(\phi - \theta) \sin(\theta)$ is transmitted to the hull causing ice resistance

$$R_T = F_T \tan(\phi - \theta) \sin(\theta) \qquad (6)$$

Where $\theta$ is the floe turning angle with respect to horizontal”

-

-

-

## Bibliography

Enkvist, E., Varsta, P. And Riska, K. (1979) The ship-ice interaction. POAC 79, page 977 to 1002. [Results from research and practical ship operation in ice, crushing, friction ridge resistance, bow shape angles and propeller-ice-interaction]

Evers, K.-U.; Jochmann, P. (1993): "An Advanced Technique to Improve the Mechanical Properties of Model Ice Developed at the HSVA Ice Tank", Proceedings of the 12'th International Conference on Port and Ocean Engineering under Arctic Conditions, Hamburg, August 17-20, 1993. [Model ice production with improved mechanical properties, air bubble introduction and scraping of the bottom side of the model ice]

Finnish Maritime Administration, Swedish Maritime Administration, (2005), Guidelines for the application of the Finnish – Swedish ice class rules, Appendix 4, Guidelines for the verification of a ship's performance for ice classes through model ice [Ice class rules, Appendix 4: detailed rules for carrying out brash ice model tests]

Haase A., Solange Van Der Werft, Jochmann P., (2012), DYPIC – Dynamic Positioning in ice – first phase of model testing, Proceeding of the ASME 2012 31th International Conference on Ocean, Offshore and Arctic Engineering OMAE 2012, July 1-6, 2012 Rio de Janeiro, Brazil [Dynamic positioning system for a model ice basin, first step]

Haase A., Jochmann P., (2013), DYPIC – Dynamic Positioning in ice – second phase of model testing, Proceeding of the ASME 2013 32nd International Conference on Ocean, Offshore and Arctic Engineering OMAE 2013, June 9-14, 2013 Nantes, France [Dynamic positioning system for a model ice basin, results and tests]

Hellmann J.-H., Rupp K.-H., Evers K.-U., Hansen R., Schwarz J., And Hoffmann L., (1988) Ice Trials with the Soviet Icebreaker Mudyug after Conversion to the Thyssen-Waas Icebreaking System, Spitsbergen April 1987. HSVA Report [Ice trial report in level ice, snow free level ice, ridges and maneuvering in ice]

HSVA Hamburg Ship Model Basin, Preparation of Model Ice, Ice Technology at HSVA (2010), on request at HSVA [Description of ice and ice tests at the Hamburg Ship Model Basin]

ITTC International Towing Tank Conference, ITTC – Recommended Procedures and Guidelines (2011), Testing and Extrapolation Methods, Ice Testing, Chapters:

- General Guidelines
- Resistance Tests in Level Ice
- Manoeuvring Tests in Ice
- Test Methods for Model Ice Properties
- Propulsion Tests in Ice
- Tests in Deformed Ice

Kämäräinen J., (1993), Evaluation of ship ice resistance calculation methods, Helsinki University of Technology, Faculty of Mechanical Engineering, February19, 1993 [Analysis of ice resistance with the influence of ice thickness, ice bending strength and ice friction. Comparison of empirical level ice resistance calculation methods and comparison of the ice resistance calculation methods with full scale data]

Kämäräinen J., (2007), Theoretical Investigation on the Effect of Fluid Flow Between the Hull of a Ship and Ice Floes on the Resistance in Level Ice, Doctoral Dissertation, TKK Dissertation 80, Helsinki University of Technology [Calculation of the low pressure between ice floes and ship surface, hydrodynamic lubrication theory]

Kayo Y., (1993) Measurement of Ice Load Distribution on an Icebreaker Bow Model Composed by Load Panels. The 12th International Conference on Port and Ocean Engineering under Arctic Conditions (POAC), Hamburg, Volume 1, page 328-337. [Segmented ship model tests for studying the ice breaking events, the load distribution and floe movement over the hull]

Keinonen A.J., Browne R.P., Revill C.R., (1991), TP 10923 E, Icebreaker Design Synthesis Phase 2, Analysis of Contemporary Icebreaker Performance, Prepared for: Transportation Development Centre, Policy and Coordination Group, Transport Canada, September 1991 [Full scale performance data of icebreakers, the influence of hull shape and the different ice conditions]

Keinonen A., Browne R.P. Rewill C.R. And Bayly I.M. (1991), Icebreaker Performance Prediction. SNAME Annual Meeting, New York, Nov. 13-16, 1991, p. 7-1 – 7-21 [Full scale performance data of icebreakers, the influence of hull shape and the different ice conditions]

Kotras; J.W., Baird, A.V. And Naege, J.N. (1983), Predicting ship performance in level ice, *Transactions SNAME*, Vol. 91. [Ice breaking and empirical prediction of ship performance in ice]

Liukkonen S. (1989), About Physical Modelling of Kinetic Friction between Ice and Ship, *POAC* 89, p. 736-749 [Friction measurements in model and full scale. Study of various parameters affecting ice friction]

Puntigliano F.M. (2000). Ice Performance of the MPV Neuwerk. On the Low Pressure Phenomenon between Ice and Hull, Full-Scale Trials, Physical and Mathematical Modelling. HSVA Report No. 1640 Part B. [Results of the full scale measurement of the low pressure phenomenon on board of the German MPV NEUWERK]

Puntigliano F.M. (2003). Experimental and Numerical Research on the Interaction

Between Ice Floes and a Ship's Hull during Icebreaking. (2003) TU Hamburg - Harburg Schriftenreihe Schiffbau, September 2003, Bericht 622. [Low pressure phenomenon measured in full scale and model scale, theoretical calculations]

Valanto P. (2001). The Resistance of Ships in Level Ice. *SNAME Transactions*, Vol. 109, 2001, 53 – 83. [Numerical 3-D model of the ice breaking process at the ship waterline for investigating resistance forces on ship hulls.]

Valanto P. (2001), *Compendium of ship hydrodynamics, Part X: Hydrodynamics of special vehicles, Chapter 24: Icebreaking and ice strengthened ships*, Presses de l'ENSTA, 2013 to be published [History, physical mechanisms, experimental data and methods, semi-empirical formulas, icebreaking resistance and hull form]

## Biographical Sketch

**Karl-Heinz Rupp** started his seafaring carrier in 1964, visited the Nautical Academy from 1968 to 1971 and received the German master licence for all ships. He studied naval Architecture at the University of Hannover and Hamburg (certificated engineer (Dipl. Ing.)) and graduated as Dr.-Ing in 1984 from the University of Hannover.

From 1984 to 2012 he worked as a research engineer at the Hamburg Ship Model Basin (HSVA) as a project leader for developing and model testing of:

Icebreakers and icebreaking research vessels
Icebreaking transportation vessels
Icebreaking inshore vessels for shallow draft and
Drilling vessels in ice

Dr. Rupp was a participant, observer, project leader and task leader in several full scale trials and voyages in arctic and other ice covered regions.